MISTA candidate magnetic field models for IGRF-14

Keke Zhang[1], Hongbo Yao[1], Qing Yan[1], Yi Jiang[1], Pengfei Liu[1], Liang Yin[1], Juyuan Xu[1], Zhengyong Ren[2], Yufeng Lin[3], Yan Feng[4], Yongxin Pan[5]

[1]Macau Institute of Space Technology and Application, Macau University of Science and Technology, Macao, China

[2]School of Geosciences and Info-Physics, Central South University, Changsha, China

[3]Department of Earth and Space Sciences, Southern University of Science and Technology, Shenzhen, China

[4] Institute of Space Weather, Nanjing University of Information Science & Technology, Nanjing, China

[5] Institute of Geology and Geophysics, Chinese Academy of Sciences, Beijing, China

1. Introduction

This document reports the data and methods used to construct the Macau Institute of Space Technology and Application (MISTA) candidate magnetic field models for the 14th generation International Geomagnetic Reference Field (IGRF-14). Based on the latest magnetic data from Macau Science Satellite-1 (MSS-1), Swarm satellites, and observatories, we provide three candidate magnetic field models for IGRF-14:

(1) DGRF-2020: Internal field (main field) for 2020.0 to SH degree and order 13 (which is based on the Swarm and observatory data because MSS-1 data were not available in 2020).

(2) IGRF-2025: Internal field (main field) for 2025.0 to spherical harmonic (SH) degree and order 13 (which is based on the MSS-1, Swarm, and observatory data).

(3) SV-2025-2030: Predicted average secular variation for 2025.0-2030.0 to SH degree and order 8 (which is based on the MSS-1, Swarm, and observatory data).

2. Data

2.1 Satellite data

We used satellite magnetic data measured by MSS-1 and Swarm satellites. For the Swarm satellite, we utilized both vector and scalar data from January 1, 2014, to August 31, 2024. For the MSS-1

satellite, we utilized vector data from November 1, 2023, to August 31, 2024. All data are resampled to 1-minute interval. Like the CHAOS geomagnetic field model series (Finlay et al., 2020; Olsen et al., 2006), the following data selection criteria are applied to select dark-region and geomagnetically quiet-time data:

(1) Dark region only (sun at least 10° below the horizon).

(2) The 3-hour planetary K index $Kp \leq 2^{o}$.

(3) The magnetospheric ring current index RC changes by at most 2nT/h, $|dRC/dt| \leq 2\text{nT/h}$.

(4) The merging electric field E_m averaged over the previous 2h is no more than 0.8 mV/m, i.e., $E_m \leq 0.8\text{mV/m}$.

(5) Interplanetary magnetic field (IMF) B_z averaged over the previous 2h is positive.

(6) Vector data were used at the equatorward of 55° quasi-dipole latitude, and scalar data were used at the poleward of 55° quasi-dipole latitude.

Figure 1 illustrates the monthly number of MSS-1 and Swarm magnetic data points during January 1, 2020 and August 31, 2024. Figure 2 shows the spatial distribution of MSS-1 and Swarm magnetic data points during November 1, 2023 and August 31, 2024. After data selection, the total numbers of vector and scalar satellite data points are 974,299 and 329,315, respectively.

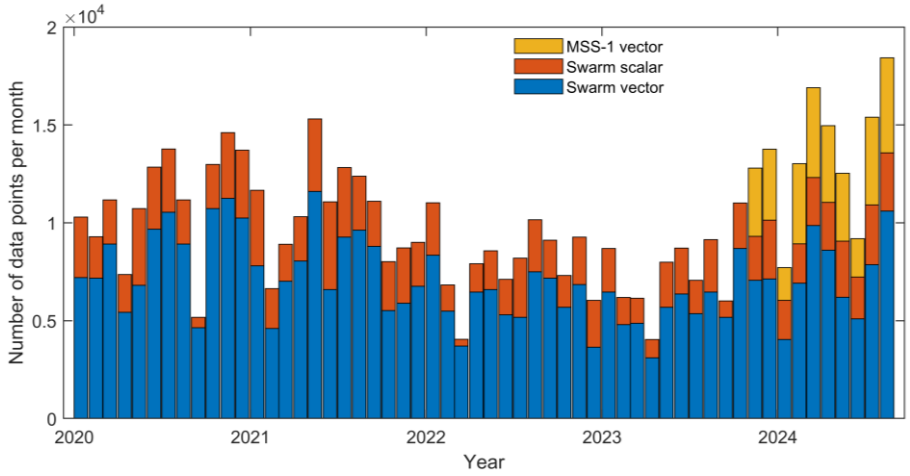

Figure 1. Illustration of the monthly number of MSS-1 and Swarm magnetic data points during January 1, 2020 and August 31, 2024.

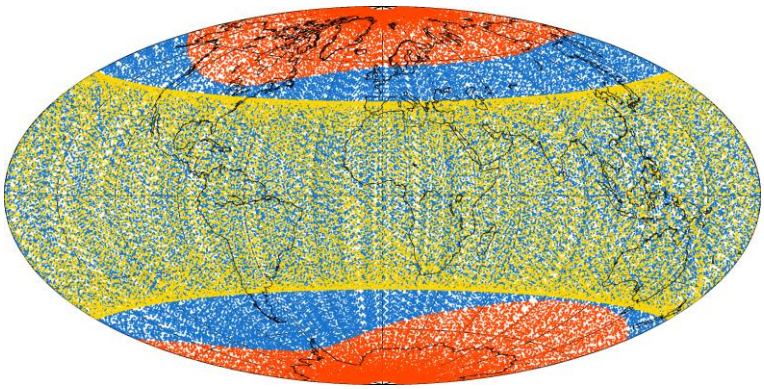

Figure 2. Spatial distribution of MSS-1 (yellow) and Swarm (blue for vector, orange for scalar) magnetic data points during November 1, 2023 and August 31, 2024.

2.2 Observatory data

To better constrain the secular variation of core field, we also used annual differences of revised monthly means of observatory data (Olsen et al., 2014). Here, annual differences of revised monthly means were derived from hourly mean values of 163 geomagnetic observatories from 2013 to 2024 (Macmillan & Olsen, 2013). Figure 3 shows the location of the 163 geomagnetic observatories. Annual differences of revised monthly means were calculated as follows. First, ionospheric primary and induced fields as predicted by the CM6 geomagnetic field model (Sabaka et al., 2020) and magnetospheric primary and induced fields as predicted by the CHAOS-7 geomagnetic field model (Finlay et al., 2020) were subtracted from observatory hourly values. Second, revised monthly means were calculated using Huber-weighted robust method. Finally, annual differences of revised monthly means at time t were calculated by $B(t+6\text{months})-B(t-6\text{months})$, where B can be radial component B_r, colatitude component B_θ, and longitude component B_ϕ.

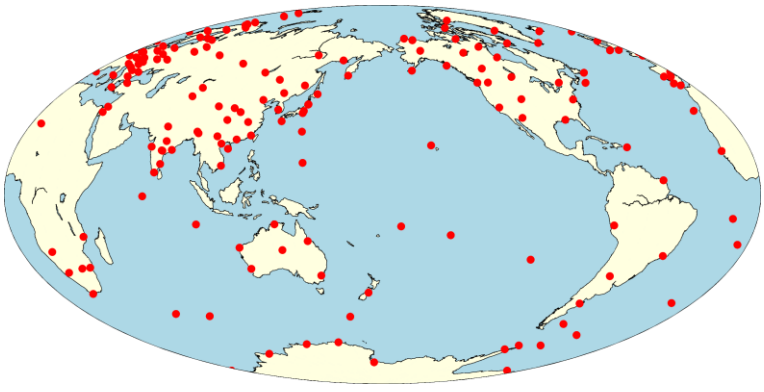

Figure 3. Location of the 163 geomagnetic observatories.

3. Geomagnetic field modeling

3.1 Model parametrization

For accurate IGRF-type main field modeling, we co-estimate the core field, smaller spatial scale crustal field, and magnetospheric field. In source-free regions, the magnetic field $\mathbf{B} = -\nabla V$ is derived from a magnetic scalar potential V, which consists of an internal part V^{int} for core and crustal fields, and an external part V^{ext} for magnetospheric and their Earth-induced fields. The internal potential V^{int} is described with spherical harmonic (SH) model

$$V^{\text{int}} = a\sum_{n=1}^{N_{\text{int}}}\sum_{m=0}^{n}(g_n^m \cos m\phi + h_n^m \sin m\phi)\left(\frac{a}{r}\right)^{n+1} P_n^m(\cos\theta), \quad (1)$$

where $a = 6371.2$ km is the Earth's mean radius, r, θ, and ϕ are the radius, colatitude, and longitude, respectively. $P_n^m(\cos\theta)$ is the Schmidt quasi-normalized associated Legendre function of degree n and order m (Winch et al., 2005), $N_{\text{int}} = 50$ is the maximum degree used to describe the internal field, g_n^m and h_n^m are the model coefficients. Consistent with the CHAOS-7 geomagnetic field model (Finlay et al., 2020), core field is determined up to degree $n = 20$ with time variations are represented by order 6 B-splines (de Boor, 2001). Static crustal field is determined for degrees $n = 21 - 50$. Large-scale magnetospheric primary and induced fields are determined up to degree $n = 2$ (Olsen et al., 2014).

3.2 Model estimation

Like the CHAOS geomagnetic field model series (Finlay et al., 2020; Olsen et al., 2014), we minimizing the following objective function to estimate the model parameters $\mathbf{m}$

$$\phi(\mathbf{m}) = \mathbf{e}^T\mathbf{C}_d^{-1}\mathbf{e} + \lambda_3\mathbf{m}^T\mathbf{\Lambda}_3\mathbf{m} + \lambda_2\mathbf{m}^T\mathbf{\Lambda}_2\mathbf{m}, \quad (2)$$

where $\mathbf{e} = \mathbf{d}_{\text{obs}} - \mathbf{d}_{\text{mod}}$ is the data residual vector, $\mathbf{d}_{\text{obs}}$ is measured magnetic data vector, $\mathbf{d}_{\text{mod}}$ are model predictions, $\mathbf{C}_d^{-1}$ is the inverse of the data error covariance matrix considering the anisotropic errors due to attitude uncertainty (Olsen, 2002). $\mathbf{\Lambda}_3$ and $\mathbf{\Lambda}_2$ are the block diagonal damping matrices that constrain the third and second-time derivatives of the core field, respectively(Olsen et al.,

2014). $\lambda_3 = 0.33(\mathrm{nTyr}^{-3})^{-2}$ and $\lambda_2 = 100(\mathrm{nTyr}^{-2})^{-2}$ (Finlay et al., 2015) control the strength of damping; to reduce the effect of unmodelled external fields, all zonal terms g_n^0 are treated separately with λ_3 increased to $100(\mathrm{nTyr}^{-3})^{-2}$.

3.3 Extraction of IGRF candidate models

The above geomagnetic field model is the parent model of our MISTA candidate models. Our extraction of IGRF candidate models is similar to the way of the CHOAS IGRF parent models (Finlay et al., 2015, 2020):

(1) DGRF-2020

MISTA core field model was evaluated at epoch 2020.00 for SH degrees $n = 1-13$ and was output in 0.01nT precision.

(2) IGRF-2025

MISTA core field model g_n^m was evaluated at epoch 2024.75 for SH degrees $n = 1-13$, SV field model $\dot{g}$ was evaluated at epoch 2024.00 for SH degrees $n = 1-13$, the core field model at epoch 2025.00 was evaluated by

$$g_n^m(t_{2025.00}) = g_n^m(t_{2024.75}) + 0.25year \cdot \dot{g}(t_{2024.00}) \tag{3}$$

(3) SV-2025-2030

As the predicted average secular variation for 2025.0-2030.0, MISTA SV field model was evaluated at epoch 2024.00 for SH degrees $n = 1-8$ and was output in 0.01nT precision.

4. MISTA candidate magnetic field models for IGRF-14

4.1 Residual statistics and data fit

Table 1. Residual statistics of MISTA candidate magnetic field models for IGRF-14

Data	Component	Number of data	Mean	RMS
Swarm-A	F	157858	-0.10	3.54
	B_r	312848	0.10	1.80
	B_θ	312848	0.07	2.59
	B_ϕ	312848	0.06	2.18

Swarm-B	F	156700	0.07	3.34
	B_r	311828	-0.03	1.80
	B_θ	311828	-0.06	2.60
	B_ϕ	311828	0.04	2.28
Swarm-C	F	14757	0.03	2.95
	B_r	313465	0.14	1.84
	B_θ	313465	-0.02	2.61
	B_ϕ	313465	-0.23	2.25
MSS-1	B_r	36158	-0.01	2.32
	B_θ	36158	0.39	3.29
	B_ϕ	36158	-0.07	2.93
Observatory	dB_r / dt	13387	-0.01	3.05
	dB_θ / dt	13387	0.11	3.15
	dB_ϕ / dt	13387	-0.02	2.53

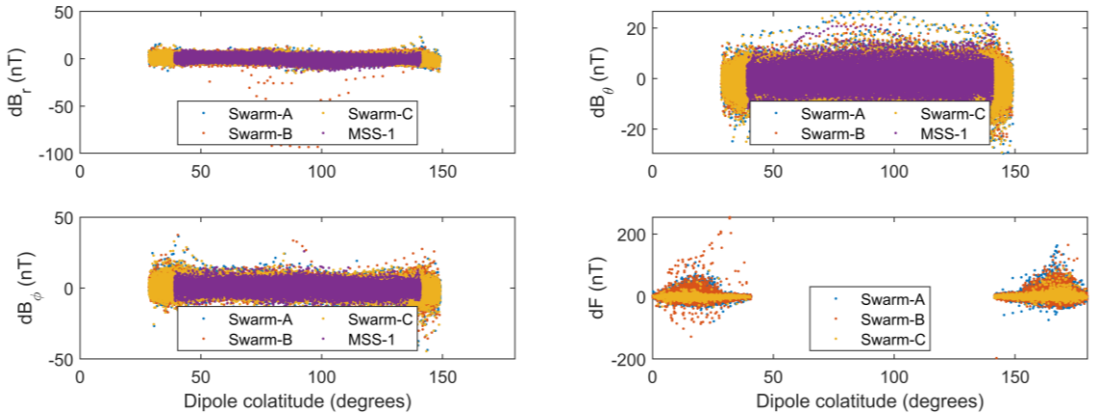

Figure 4. Residuals between MISTA model prediction and MSS-1 and Swarm satellite magnetic data

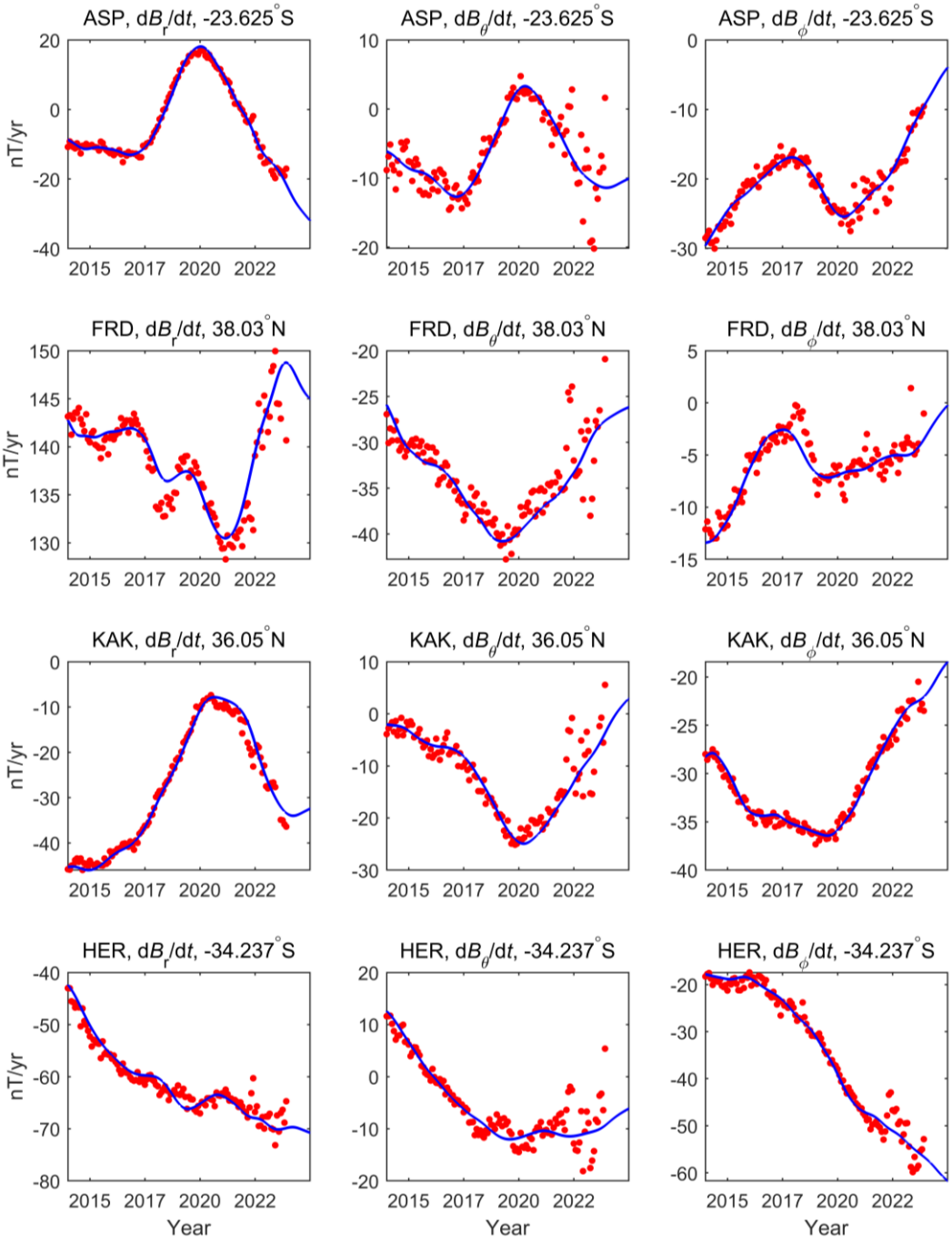

Figure 5. Fit of MISTA model prediction (blue line) to the annual differences of revised monthly means (red dot) at example geomagnetic observatories.

4.2 IGRF-13's DGRF-2015 validation and IGRF-14's DGRF-2020 candidate

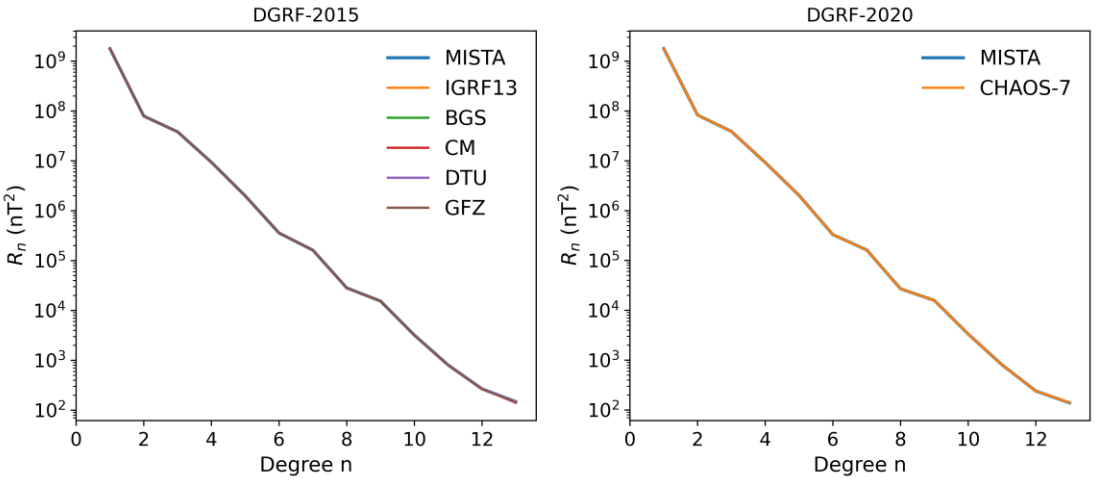

Figure 6. Spherical harmonic spectra of the DGRF-2015 validation model (left) and the DGRF-2020 candidate model (right).

4.3 IGRF-13's IGRF-2020 validation and IGRF-14's IGRF-2025 candidate

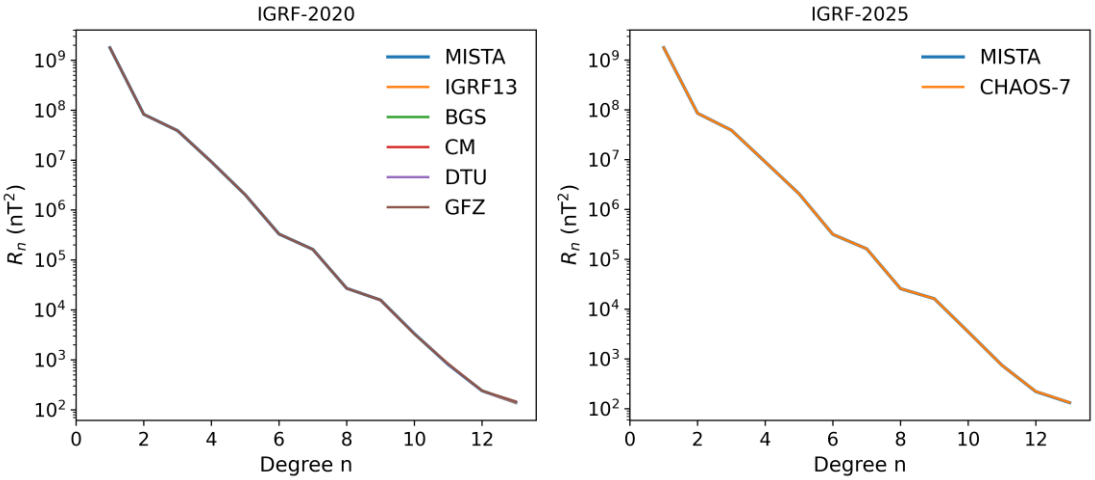

Figure 7. Spherical harmonic spectra of the IGRF-2020 validation model (left) and the IGRF-2025 candidate model (right).

4.4 IGRF-13's SV-2020-2025 validation and IGRF-14's SV-2025-2030 candidate

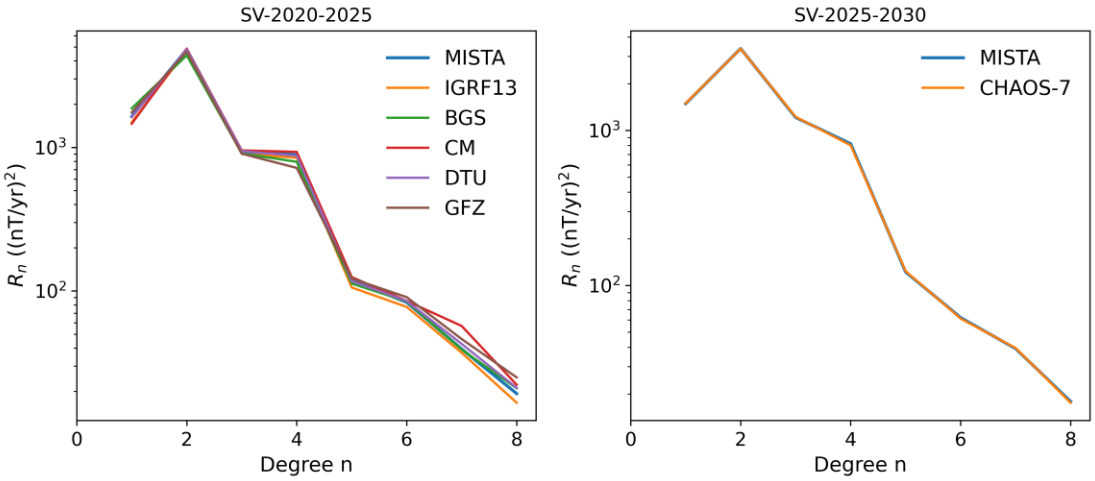

Figure 8. Spherical harmonic spectra of the SV-2020-2025 validation model (left) and the SV-2025-2030 candidate model (right).

5. Conclusions

We have derived the MISTA candidate magnetic field models for IGRF-14 using MSS-1, Swarm, and annual differences of revised monthly means of observatory data. Our candidate magnetic field models include (1) main field for 2020.0 to SH degree and order 13 (DGRF-2020); (2) main field for 2025.0 to SH degree and order 13 (IGRF-2025); and (3) predicted average secular variation for 2025.0-2030.0 to SH degree and order 8 (SV-2025-2030). Comparison with published IGRF-13 candidate models and DTU's CHAOS-7 model conformed the reliability and accuracy of our models.

Acknowledgments

This work was financially supported by the National Natural Science Foundation of China (42250101) and the Macao Foundation.

References

de Boor, C. (2001). A Practical Guide to Splines. In *Springer*. Springer. https://www.jstor.org/stable/2006241?origin=crossref

Finlay, C. C., Kloss, C., Olsen, N., Hammer, M. D., Tøffner-Clausen, L., Grayver, A., & Kuvshinov, A. (2020). The CHAOS-7 geomagnetic field model and observed changes in the South Atlantic Anomaly. *Earth, Planets and Space*, *72*(1), 156. https://doi.org/10.1186/s40623-020-01252-9

Finlay, C. C., Olsen, N., & Tøffner-Clausen, L. (2015). DTU candidate field models for IGRF-12 and

the CHAOS-5 geomagnetic field model. *Earth, Planets and Space*, *67*(1), 114. https://doi.org/10.1186/s40623-015-0274-3

Macmillan, S., & Olsen, N. (2013). Observatory data and the Swarm mission. *Earth, Planets and Space*, *65*(11), 1355–1362. https://doi.org/10.5047/eps.2013.07.011

Olsen, N. (2002). A model of the geomagnetic field and its secular variation for epoch 2000 estimated from Ørsted data. *Geophysical Journal International*, *149*(2), 454–462. https://doi.org/10.1046/j.1365-246X.2002.01657.x

Olsen, N., Lühr, H., Finlay, C. C., Sabaka, T. J., Michaelis, I., Rauberg, J., & Tøffner-clausen, L. (2014). The CHAOS-4 geomagnetic field model. *Geophysical Journal International*, *197*(2), 815–827. https://doi.org/10.1093/gji/ggu033

Olsen, N., Lühr, H., Sabaka, T. J., Mandea, M., Rother, M., Tøffner-Clausen, L., & Choi, S. (2006). CHAOS - A model of the Earth's magnetic field derived from CHAMP, Ørsted, and SAC-C magnetic satellite data. *Geophysical Journal International*, *166*(1), 67–75. https://doi.org/10.1111/j.1365-246X.2006.02959.x

Sabaka, T. J., Tøffner-Clausen, L., Olsen, N., & Finlay, C. C. (2020). CM6: a comprehensive geomagnetic field model derived from both CHAMP and Swarm satellite observations. *Earth, Planets and Space*, *72*(1), 80. https://doi.org/10.1186/s40623-020-01210-5

Winch, D. E., Ivers, D. J., Turner, J. P. R., & Stening, R. J. (2005). Geomagnetism and Schmidt quasi-normalization. *Geophysical Journal International*, *160*(2), 487–504. https://doi.org/10.1111/j.1365-246X.2004.02472.x